

# Yeast Surface Display of Trifunctional Minicellulosomes for Simultaneous Saccharification and Fermentation of Cellulose to Ethanol<sup>∇†</sup>

Fei Wen,<sup>1</sup> Jie Sun,<sup>1,2</sup> and Huimin Zhao<sup>1,3\*</sup>

Department of Chemical and Biomolecular Engineering, University of Illinois at Urbana-Champaign, 600 South Mathews Avenue, Urbana, Illinois 61801<sup>1</sup>; Department of Biological Engineering, East China University of Science and Technology, Shanghai, China<sup>2</sup>; and Departments of Chemistry, Biochemistry, and Bioengineering, Institute for Genomic Biology, Center for Biophysics and Computational Biology, University of Illinois at Urbana-Champaign, 600 South Mathews Avenue, Urbana, Illinois 61801<sup>3</sup>

Received 16 July 2009/Accepted 7 December 2009

**By combining cellulase production, cellulose hydrolysis, and sugar fermentation into a single step, consolidated bioprocessing (CBP) represents a promising technology for biofuel production. Here we report engineering of *Saccharomyces cerevisiae* strains displaying a series of uni-, bi-, and trifunctional minicellulosomes. These minicellulosomes consist of (i) a miniscaffoldin containing a cellulose-binding domain and three cohesin modules, which was tethered to the cell surface through the yeast  $\alpha$ -agglutinin adhesion receptor, and (ii) up to three types of cellulases, an endoglucanase, a cellobiohydrolase, and a  $\beta$ -glucosidase, each bearing a C-terminal dockerin. Cell surface assembly of the minicellulosomes was dependent on expression of the miniscaffoldin, indicating that formation of the complex was dictated by the high-affinity interactions between cohesins and dockerins. Compared to the unifunctional and bifunctional minicellulosomes, the quaternary trifunctional complexes showed enhanced enzyme-enzyme synergy and enzyme proximity synergy. More importantly, surface display of the trifunctional minicellulosomes gave yeast cells the ability to simultaneously break down and ferment phosphoric acid-swollen cellulose to ethanol with a titer of  $\sim 1.8$  g/liter. To our knowledge, this is the first report of a recombinant yeast strain capable of producing cell-associated trifunctional minicellulosomes. The strain reported here represents a useful engineering platform for developing CBP-enabling microorganisms and elucidating principles of cellulosome construction and mode of action.**

Alternatives to fossil fuels for transportation are under extensive investigation due to the increasing concerns about energy security, sustainability, and global climate change (22, 24, 35). Lignocellulosic biofuels, such as bioethanol, have been widely regarded as a promising and the only foreseeable alternative to petroleum products currently used in transportation (11, 35, 39, 41). The central technological impediment to more widespread utilization of lignocellulose is the absence of low-cost technology to break down its major component, cellulose (19, 41). Cellulose (a linear homopolymer of glucose linked by  $\beta$ -1,4-glycosidic bonds) is insoluble, forms a distinct crystalline structure, and is protected by a complex plant cell wall structural matrix (10, 32). As a result, a separate processing step is required to produce large amounts of cellulases for the hydrolysis of cellulose into fermentable glucose, which makes cellulosic ethanol too expensive to compete with gasoline. Therefore, consolidated bioprocessing (CBP), which combines enzyme production, cellulose hydrolysis, and fermentation in a single step, has been proposed to significantly lower the cost of cellulosic ethanol production (23, 24). However, the great potential of CBP cannot be realized using microorganisms available today.

One engineering strategy to construct CBP-enabling microbes is to endow ethanologenic microorganisms, such as *Saccharomyces cerevisiae*, with the ability to utilize cellulose by heterologously expressing a functional cellulase system. Nature has provided two ways of designing such systems: (i) noncomplexed cellulase systems, in which free enzymes are secreted and act discretely, and (ii) complexed cellulase systems, namely, cellulosomes, in which many enzymes are held together by a noncatalytic scaffoldin protein through high-affinity interactions between its cohesins and enzyme-borne dockerins (24). By mimicking the noncomplexed cellulase system, several groups successfully constructed cellulolytic *S. cerevisiae* strains that directly ferment amorphous cellulose to ethanol, although the titer and yield were relatively low (12, 16, 17). Compared to the noncomplexed cellulase systems, the cellulosome exhibits much greater degradative potential as a result of its highly ordered structural organization that enables enzyme proximity synergy and enzyme-substrate-microbe complex synergy (2, 13, 14, 21). Therefore, the second strategy could provide a “quantum leap” in development of biomass-to-biofuel technology (3).

Recent studies revealed the modular nature of cellulosome assembly; by simply appending a dockerin domain, up to three enzymes (either cellulosomal or noncellulosomal) with different origins could be incorporated into a chimeric miniscaffoldin consisting of divergent cohesin domains to form a minicellulosome *in vitro*. The chimeric miniscaffoldin was in the form of either purified (7, 15, 26) or yeast surface-displayed protein (34). In both cases, the resulting recombinant minicellulosomes showed enhanced hydrolysis activity with cellulose.

\* Corresponding author. Mailing address: Department of Chemical and Biomolecular Engineering, University of Illinois at Urbana-Champaign, 600 South Mathews Avenue, Urbana, IL 61801. Phone: (217) 333-2631. Fax: (217) 333-5052. E-mail: zhao5@illinois.edu.

† Supplemental material for this article may be found at <http://aem.asm.org/>.

∇ Published ahead of print on 18 December 2009.

TABLE 1. Recombinant *S. cerevisiae* EBY100 strains used in the cellulose hydrolysis study

Strain <sup>a</sup>	Plasmid(s)	Phenotype
HZ1901	pYD1ctrl and pRS425	No surface display (negative control)
HZ1859 (CipA3-EGII)	pYD1-CipA3-EGII	Displays unifunctional minicellulosome with EGII activity
HZ1890 (CipA3-CBHII)	pYD1-CipA3 and pRS425-CBHII	Displays unifunctional minicellulosome with CBHII activity
HZ1900 (CipA3-BGL1)	pYD1-CipA3 and pRS425-BGL1	Displays unifunctional minicellulosome with BGL1 activity
HZ1892 (CipA3-EGII-CBHII)	pYD1-CipA3-EGII and pRS425-CBHII	Displays bifunctional minicellulosome with EGII and CBHII activities <sup>b</sup>
HZ1886 (CipA3-EGII-CBHII-BGL1)	pYD1-CipA3-EGII and pRS425-CBHII-BGL1	Displays trifunctional minicellulosome with EGII, CBHII, and BGL1 activities <sup>b</sup>
HZ1891 (CipA1-EGII-CBHII)	pYD1-CipA1-EGII and pRS425-CBHII	Displays two types of unifunctional minicellulosomes, one with EGII activity and one with CBHII activity
HZ1885 (CipA1-EGII-CBHII-BGL1)	pYD1-CipA1-EGII and pRS425-CBHII-BGL1	Displays three types of unifunctional minicellulosomes, one with EGII activity, one with CBHII activity, and one with BGL1 activity

<sup>a</sup> For clarity, in the text the strains are referred by their designations in parentheses.

<sup>b</sup> The phenotype shown assumes that all minicellulosome components are expressed at a 1:1 ratio. However, due to the relatively low level of enzyme expression, our results showed that there was a heterogeneous population of cells displaying uni-, bi-, and/or trifunctional minicellulosomes when two or three enzymes were coexpressed with CipA3.

These results indicate that the high-affinity cohesin-dockerin interactions are sufficient to dictate assembly of a functional cellulosome. Therefore, in theory, the same results could also be achieved *in vivo* by coexpressing the cellulosomal components in a recombinant host. To date, *in vivo* production of recombinant cellulosomes has been limited to unifunctional complexes containing only one type of cellulolytic enzyme (1, 8, 27). Since complete enzymatic hydrolysis of cellulose requires synergistic action of three types of cellulases, endoglucanases (EGs) (EC 3.2.1.4), exoglucanases (including cellodextrinases [EC 3.2.1.74] and cellobiohydrolases [CBHs] [EC 3.2.1.91]), and  $\beta$ -glucosidases (BGLs) (EC 3.2.1.21) (24), none of the engineered microorganisms were shown to utilize cellulose directly.

In this study, we report the first successful assembly of trifunctional minicellulosomes in *S. cerevisiae*. The resulting recombinant strain was able to simultaneously hydrolyze and ferment amorphous cellulose to ethanol, demonstrating the feasibility of constructing cellulolytic and fermentative yeasts by displaying recombinant minicellulosomes on the cell surface. We chose the cell surface display format over secretory proteins to potentially incorporate the cellulose-enzyme-microbe complex synergy unique to native cellulolytic microorganisms (21). Coupled with flow cytometry, yeast surface display provides a more convenient engineering platform, avoiding labor-intensive protein purification steps. Such a cell-bound format is also amenable to analysis of enzyme activity with insoluble substrates (31). Therefore, the system described here could be a useful tool for studying and engineering recombinant cellulosomes for various industrial and biotechnological applications.

#### MATERIALS AND METHODS

**Strains, media, and reagents.** *S. cerevisiae* EBY100 (Invitrogen, Carlsbad, CA) was used for yeast cell surface display, and the recombinant yeast strains are summarized in Table 1. *Escherichia coli* DH5 $\alpha$  (Cell Media Facility, University of Illinois at Urbana-Champaign, Urbana, IL) was used for recombinant DNA

manipulation. *Clostridium thermocellum* DSM1237, *Trichoderma reesei* DSM769, and *Aspergillus aculeatus* DSM2344 were purchased from DSMZ (Braunschweig, Germany). *S. cerevisiae* EBY100 transformants were selected and maintained on SC-Trp, SC-Leu, or SC-Trp-Leu plates (0.167% yeast nitrogen base without amino acids and ammonium sulfate [Difco Laboratories, Detroit, MI], 0.5% ammonium sulfate, 2% glucose, 1.5% agar, and appropriate supplements) and were induced in YPG (1% yeast extract, 2% peptone, 2% galactose). *E. coli* was cultured in LB medium (Fisher, Pittsburgh, PA). *C. thermocellum* was cultured anaerobically in reinforced clostridial medium (Difco) supplemented with 0.6% cellobiose. *T. reesei* and *A. aculeatus* were grown on YPAD plates (1% yeast extract, 2% peptone, 2% glucose, 0.01% adenine hemisulfate, 1.5% agar). All restriction enzymes were obtained from New England Biolabs (Ipswich, MA). Unless otherwise indicated, all chemicals were purchased from Sigma (St. Louis, MO).

**Plasmid construction.** The sequences of all PCR primers used are listed in Table S1 in the supplemental material. Primers were synthesized by Integrated DNA Technologies (Coralville, IA). Plasmid pYD1ctrl was created by cotransforming hybridized RemoveFor/RemoveRev double-stranded DNA (dsDNA) and XhoI/PmeI-digested pYD1 (Invitrogen) into EBY100. Genes encoding miniscaffolds CipA1 and CipA3 were obtained by performing PCR using primer pairs CipA1For/CipA1Rev and CipA3For/CipA3Rev, respectively, with *C. thermocellum* genomic DNA as the template. Plasmids pYD1-CipA1 and pYD1-CipA3 were constructed by cotransforming the CipA1 or CipA3 PCR products and XhoI/PmeI-digested pYD1 into EBY100. Construction of all other plasmids involved use of either the DNA assembler method described elsewhere (33) or the conventional homologous recombination method, which assembles a large DNA fragment by splicing PCR (20) and cotransformation with a linearized vector. Both methods required preparation of several PCR fragments, and the templates, primer pairs, and PCR products used for each assembly are shown in Table S2 in the supplemental material. PCR fragments F0 to F5 were spliced and ligated into BsaXI/EcoRI-digested pYD1 to assemble a GAL1-10-prepro-ADH1 expression cassette (G10A1), which was then transferred into pRS425 (New England Biolabs, Beverly, MA) between SacI and HindIII sites for protein expression. Plasmid pRS425-CBHII was obtained by cotransforming FLAG-CBHII, docS, and EagI/NdeI-digested pRS425-G10A1 into EBY100. Plasmids pRS425-EGII and pRS425-BGL1 were obtained by cotransforming EGII-ctrl and BGL1-ctrl, respectively, with HindIII/SacI-digested pRS425 into EBY100. Plasmid pRS425-CBHII-BGL1 was obtained by cotransforming G1A2-HR1, c-Myc-BGL1, docAt, ADH2, and ApaI-digested pRS425-CBHII. Plasmid pYD1-CipA1(3)-EGII was obtained by cotransforming G10A1-HR1, G10A1-HR2, G10A1-HR3, G10A1-HR4, HisG-EGII, and DrdI/NheI-digested pYD1-CipA1(3) into EBY100. All plasmids were purified from *S. cerevisiae* and then transformed into DH5 $\alpha$ , recovered, and confirmed by DNA sequencing.

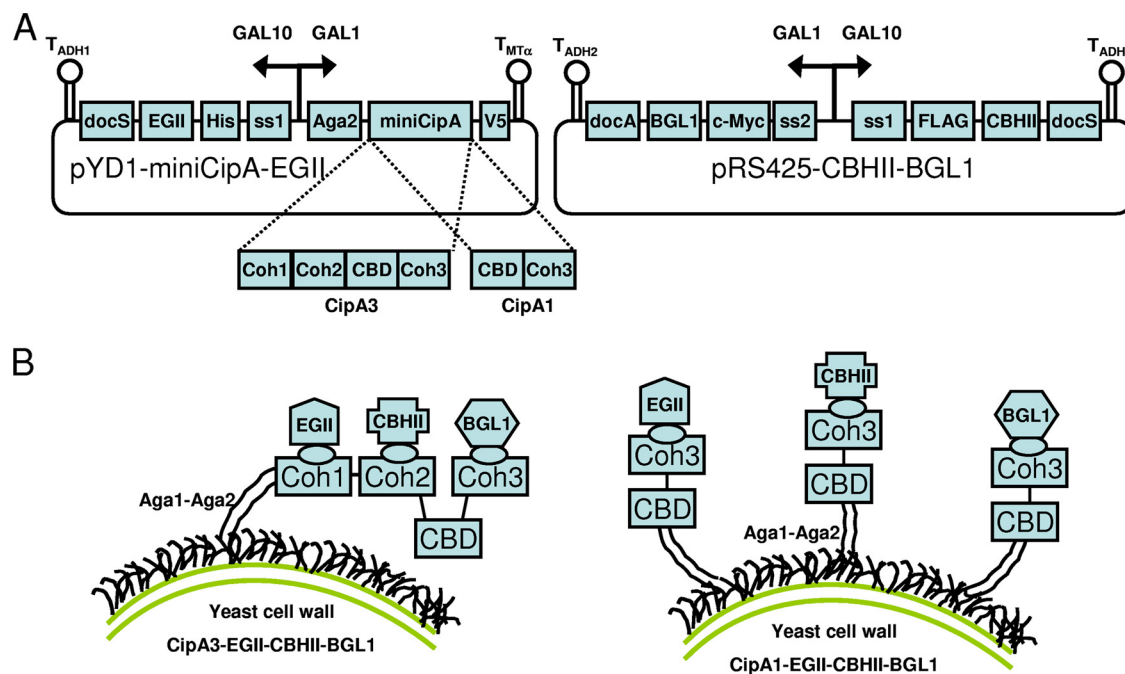


FIG. 1. Design of a yeast surface display system for assembly of minicellulosomes. (A) Plasmids used for constructing strains CipA3-EGII-CBHII-BGL1 and CipA1-EGII-CBHII-BGL1. *ss1*, synthetic prepro signal peptide (9); *ss2*,  $\alpha$ -factor signal peptide with AG dipeptide spacer (30); T, terminator. *V5* (GKPIPNPLLGLDST), *His* (HHHHHH), *FLAG* (DYKDDDDK), and *c-Myc* (EQKLISEEDL) are epitope tags used for detection of minicellulosomal components on the yeast surface. The dockerin modules, *docS* and *docA*, were obtained from the two major cellulosomal cellulases of *C. thermocellum*, *CelS* (37) and *CelA* (4), respectively. (B) Two different minicellulosome display schemes using CipA3 (left panel) and CipA1 (right panel). CipA3 enables display of trifunctional minicellulosomes, and CipA1 enables codisplay of three unifunctional minicellulosomes. The cohesin domains are numbered as described elsewhere (29). CBD, cellulose-binding domain; Coh, cohesin.

**Yeast surface display and flow cytometry analysis.** *S. cerevisiae* EBY100 clones transformed with different plasmid constructs were cultured, induced for 48 h or 72 h, and analyzed using flow cytometry as described elsewhere (38), except that only  $2.5 \times 10^6$  cells were used in each staining assay. The primary monoclonal mouse antibodies used in the assay were anti-V5 (Invitrogen), anti-His (Sigma), anti-FLAG (Sigma), and anti-c-Myc (Invitrogen) with 100-fold dilution. Quantification of the level of surface expression of the miniscaffoldin was carried out using a Quantum FITC MESF microsphere kit (Bangs Laboratories, Inc., Fishers, IN) and anti-V5-fluorescein isothiocyanate monoclonal antibody (Invitrogen) by following the manufacturer's protocol. Since the clonal variation in the level of enzyme expression was small (see Fig. 3A), a single clone was analyzed in triplicate in the enzyme activity assay and fermentation study.

**Enzyme activity assays.** Phosphoric acid-swollen cellulose (PASC) was generated from Avicel PH-101 crystalline cellulose as described elsewhere (42) and was washed at least 10 times to remove any soluble sugars. The concentrations and number-average degrees of polymerization of the substrates (PASC and Avicel) were determined using the phenol-sulfuric acid method and the modified 2,2'-bichinchoninate method as described elsewhere (40, 43). Yeast transformants displaying different minicellulosomes on the cell surface were analyzed to determine their abilities to hydrolyze PASC and Avicel. After induction in YPG, cells were washed twice with hydrolysis buffer (50 mM sodium acetate, pH 5.0) to prevent medium carryover and were resuspended in hydrolysis buffer supplemented with 0.1% PASC or Avicel to obtain an optical density at 600 nm ( $OD_{600}$ ) of  $\sim 10$ . Hydrolysis reactions were carried out in serum bottles at 30°C with agitation at 100 rpm, and 2-ml reaction samples were removed at the indicated time intervals. The amount of reducing sugar released from the insoluble substrates was measured using the Somogy-Nelson method as described elsewhere (40), and the concentrations of total sugar, total soluble sugar, and cell-derived sugar were quantified using the phenol-sulfuric acid method (40). The concentration of residual insoluble sugar was obtained by subtracting the total soluble sugar concentration and the concentration of cell-derived sugar from the total sugar concentration. All sugar concentrations were expressed as glucose equivalents. The supernatant was analyzed to determine the hydrolysis products using a high-performance liquid chromatograph (HPLC) equipped with a low-temperature evaporative light-scattering detector (Shimadzu, Columbia,

MD). Separation was carried out using a Prevail carbohydrate ES column (Alltech Associates, Inc., Deerfield, IL) at 32°C and a gradient mobile phase (80 to 65% [vol/vol] acetonitrile in water in 50 min) at a flow rate of 1 ml/min.

**Fermentation.** After induction in YPG, yeast strain CipA3-EGII-CBHII-BGL1 was washed twice with YP medium (1% yeast extract, 2% peptone) and resuspended in YP medium supplemented with 0.001% ergosterol, 0.042% Tween 80, and 1% PASC or Avicel to obtain an  $OD_{600}$  of  $\sim 50$ . Yeast strain HZ1901 was used as a negative control. Fermentation was carried out anaerobically in serum bottles at 30°C with agitation at 250 rpm, and 1-ml samples were removed at the indicated time intervals. The residual total sugar concentration was determined by subtracting the concentration of cell-derived sugar from the total sugar concentration. The ethanol concentration was determined by gas chromatography using an Agilent 7890A (Agilent Inc., Palo Alto, CA) equipped with an Agilent 5975C mass selective detector and an HP-INNOWAX column (Agilent Inc.) with helium as the carrier gas (flow rate, 1 ml/min). The temperature program used for compound separation was 80°C for 2 min, increase to 150°C at a rate of 5°C/min, increase to 260°C at a rate of 25°C/min, and then 260°C for 2 min.

## RESULTS

**Design and construction of minicellulosomal components for yeast surface display.** Complete and efficient enzymatic hydrolysis of cellulose requires synergistic action of at least three types of cellulases. Therefore, a trifunctional minicellulosome, which consists of a miniscaffoldin, an endoglucanase (EG), a cellobiohydrolase (CBH), and a  $\beta$ -glucosidase (BGL), is the minimum structure required for cellulose utilization by yeast. In this study, two miniscaffoldins, CipA3 and CipA1 (Fig. 1), were engineered based on the well-characterized scaffoldin protein CipA from *C. thermocellum* (18). CipA3, containing a cellulose-binding domain (CBD) and three cohesin

modules (Coh1-Coh2-CBD-Coh3), was designed to assemble minicellulosomes with up to three enzymatic activities (Fig. 1B, left panel). CipA1, containing a CBD and a cohesin module (CBD-Coh3), was designed to assemble a spatially restricted unifunctional minicellulosome(s) on the yeast cell surface (Fig. 1B, right panel). After fusion of the gene encoding mini-CipA to the C terminus of the AGA2 protein in the yeast pYD1 display vector, the miniscaffoldin was expected to be tethered to the yeast  $\alpha$ -agglutinin mating adhesion receptor (6) and thus displayed on the cell surface (Fig. 1B).

The enzyme components used in this study, including *T. reesei* EGII and CBHII and *A. aculeatus* BGL1, had fungal origins, and all of them were functionally expressed previously in *S. cerevisiae* (16). The noncellulosomal enzymes were chosen to demonstrate the feasibility of using yeast to produce designer cellulosomes (3). To enable surface assembly of minicellulosomes, three expression cassettes, each consisting of a promoter, a secretion signal peptide, an epitope tag, a cellulase, a dockerin module, and a terminator, were assembled in pRS425 to obtain GAL10-(prepro signal peptide)-His-EGII-docS-ADH1, GAL10-(prepro signal peptide)-FLAG-CBHII-docS-ADH1, and GAL1-( $\alpha$ -factor signal peptide)-(c-Myc)-BGL1-docA-ADH2 (Fig. 1A). The dockerin modules, docS and docA, were obtained from the two major cellulosomal cellulases of *C. thermocellum*, CelS (37) and CelA (4), respectively. Upon galactose induction, the chimeric enzymes His-EGII-docS, FLAG-CBHII-docS, and/or c-Myc-BGL1-docA were expected to be secreted and interact with the cohesin domains of the miniscaffoldin on the cell surface, forming a minicellulosome (Fig. 1B). The N-terminal epitope tags enable detection of successful assembly using flow cytometry. To simultaneously produce more than two proteins (e.g., bifunctional or trifunctional minicellulosomes) with high levels of expression in yeast, bidirectional GAL1-10 promoters (25) were used to construct the expression vectors (Fig. 1A).

**Yeast surface assembly of unifunctional minicellulosomes.** Yeast surface display of the miniscaffoldin is pivotal to minicellulosome assembly since miniscaffoldin serves as the anchor for the secretory enzymes. To verify surface immobilization of mini-CipA, yeast cells transformed with either pYD1-CipA1 or pYD1-CipA3 were stained with monoclonal anti-V5 antibody and analyzed by flow cytometry. As shown in Fig. 2A, a positively stained population was detected in both cases, indicating that the full length of mini-CipA was successfully displayed on the yeast cell surface. The peak observed for the strain transformed with plasmid pYD1ctrl was the background fluorescence typical for yeast cells. By using calibration microsphere standards coated with a known amount of fluorochrome molecules, the surface display efficiencies of CipA3 and CipA1 were determined to be approximately  $1.8 \times 10^4$  and  $3 \times 10^4$  copies per cell, respectively.

To test whether unifunctional minicellulosomes could be assembled on the yeast cell surface, plasmid pRS425 encoding one of the three chimeric enzyme expression cassettes and/or pYD1-CipA1 was transformed into yeast cells. The surface display of each enzyme was monitored by measuring the expression of the corresponding N-terminal epitope tag using flow cytometry. As shown in Fig. 2B, the chimeric enzyme was detected on the cell surface only when the miniscaffoldin CipA1 was coexpressed. In the absence of the miniscaffoldin,

enzyme expression was detected in the supernatant (data not shown) but not on the cell surface, and the recombinant yeast cells showed only background fluorescence (Fig. 2B, bottom row). Compared to coexpression of EGII or CBHII, coexpression of BGL1 did not result in a significant shift in the fluorescence peak (Fig. 2B), indicating the low level of surface display of BGL1. Similar results were observed with miniscaffoldin CipA3 (Fig. 3A). To exclude the possibility that fusion of BGL1 affected the binding of docA to mini-CipA, the supernatant of the CipA3-BGL1 strain (Table 1) was analyzed by SDS-PAGE and Western blotting. Even after the supernatant was concentrated  $\sim 75$ -fold, no free BGL1 was detected using either method (data not shown), suggesting that the majority, if not all, of the secreted BGL1 bound to the cell surface. Therefore, the low level of surface display of BGL1 was a result of a low level of expression of chimeric BGL1. Taken together, these results indicated that unfunctional cellulosomes were successfully assembled on the yeast cell surface through the interaction between the dockerin domain of the secreted chimeric enzyme and the cohesin module of mini-CipA.

**Yeast surface assembly of bifunctional and trifunctional minicellulosomes.** With the success of unfunctional minicellulosome assembly, the ability of yeast cells to display more complex minicellulosomes on the surface was examined next. Two yeast strains, CipA3-EGII-CBHII and CipA3-EGII-CBHII-BGL1, were constructed to test assembly of bifunctional and trifunctional minicellulosomes, respectively (Table 1). As shown in Fig. 3, compared to the results for yeast strains CipA3-EGII, CipA3-CBHII, and CipA3-BGL1 displaying unfunctional minicellulosomes, coexpression of two chimeric enzymes in strain CipA3-EGII-CBHII caused a noticeable but not significant decrease in the levels of display of all three minicellulosomal components. However, expression of a third enzyme in strain CipA3-EGII-CBHII-BGL1 caused a dramatic decrease in the level of display of CBHII, and there was a  $>160$ -fold drop in the number of mean fluorescence units, which might have been a result of the metabolic burden imposed on the cells when we tried to produce all four proteins simultaneously. This dramatic decrease also suggested that there was an imbalance in the molar ratio of the four minicellulosomal components, which could in theory lead to three populations of yeast cells, each displaying uni-, bi-, or trifunctional minicellulosomes in the induced CipA3-EGII-CBHII-BGL1 culture.

To test this hypothesis and to measure the percentage of each population, multiantibody staining was conducted. Compared to single-antibody staining, multiantibody staining was significantly less efficient, resulting in  $\sim 22$ -,  $\sim 85$ -, and  $\sim 3.5$ -fold reductions in the percentages of the population positively stained for EGII, CBHII, and BGL1, respectively (Fig. 3B, left panel; data not shown). These reductions in the antibody staining signal were expected since three enzymatic minicellulosomal components were in close proximity to each other, resulting in steric hindrance for simultaneous access of three bulky antibody-fluorochrome conjugates. Nevertheless, both double-positive (EGII<sup>+</sup>-CBHII<sup>+</sup> in the lower right quadrant and EGII<sup>+</sup>-BGL1<sup>+</sup> in the upper left quadrant of Fig. 3B, right panel) and triple-positive (EGII<sup>+</sup>-CBHII<sup>+</sup>-BGL1<sup>+</sup> in the upper right quadrant of Fig. 3B, right panel) populations were

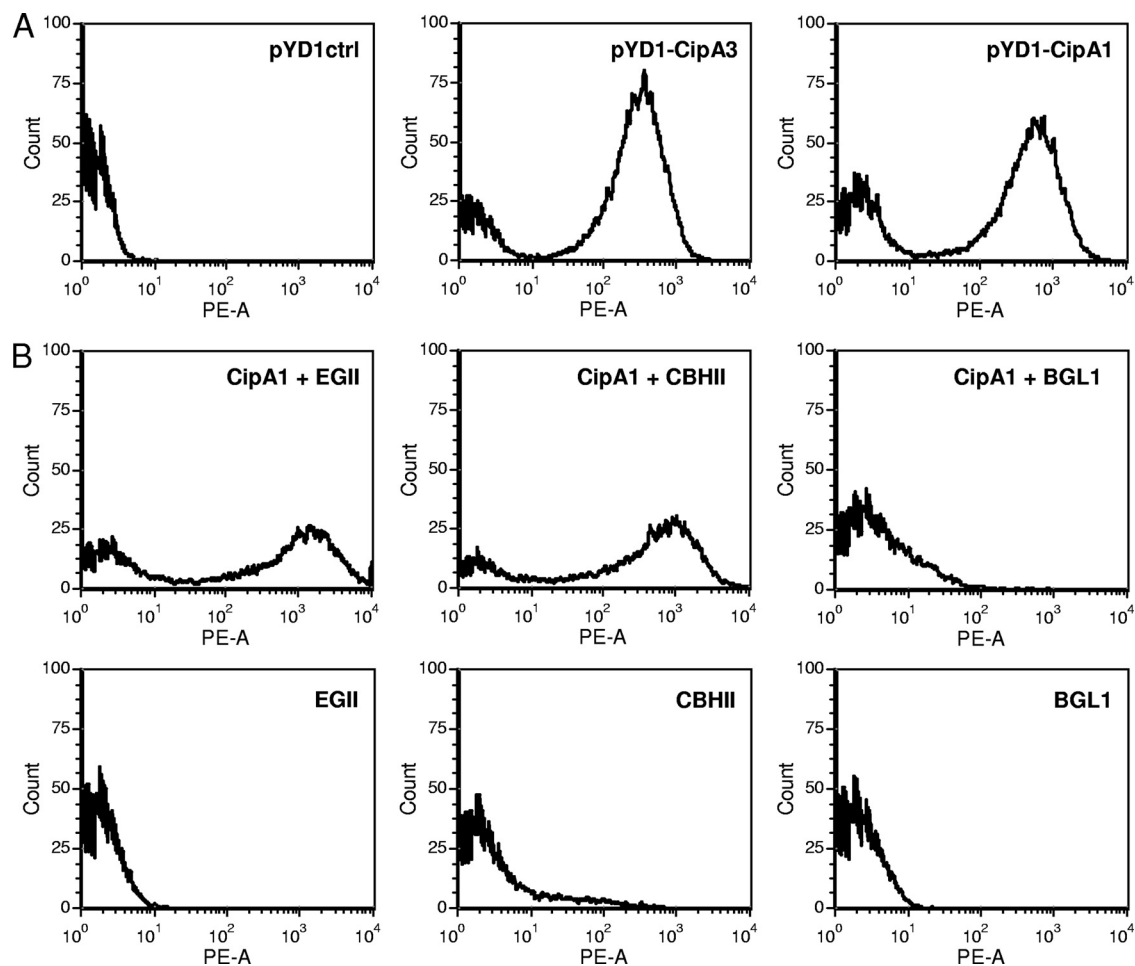


FIG. 2. Flow cytometric analysis of yeast cells displaying unifunctional minicellulosomes. (A) Both of the miniscaffoldins were successfully displayed on the yeast cell surface, as indicated by V5 epitope detection. Yeast cells transformed with empty plasmids were used as a negative control. (B) Chimeric enzyme display is dependent on the presence of the miniscaffoldin on the cell surface. With CipA1 on the surface (top row), enzymes could be detected. In contrast, without CipA1 on the surface (bottom row), no enzymes were detected on the surface. This CipA1 dependence indicated that there was successful assembly of unifunctional minicellulosomes. The results are representative of three independent experiments using three individual clones. The *x* axis (PE-A) indicates the expression levels of minicellulosomal proteins as measured by the fluorescence intensity of phycoerythrin.

detected for strain CipA3-EGII-CBHII-BGL1, indicating that a fraction of the cells displayed bifunctional ( $\sim 0.3\%$ ) and trifunctional ( $\sim 0.07\%$ ) minicellulosomes. Similar results were obtained for strain CipA3-EGII-CBHII, and a fraction ( $\sim 8.1\%$ ) of the cells displayed bifunctional minicellulosomes on the surface (Fig. 3C, upper right quadrant). It should be noted that the percentages of double- and triple-positive populations shown in Fig. 3B and 3C do not represent, and probably significantly underestimate, the true fraction size of each population due to the low efficiency of multiantibody staining.

Taken together, these data clearly suggested that the surface-displayed miniscaffoldin CipA3 and enzyme-bound dockers (docS and docA) were all correctly folded and that their high-affinity interactions were sufficient to direct assembly of a series of bi- and trifunctional minicellulosomes on the yeast cell surface, although a fraction of the cells also displayed minicellulosomes with a lesser complexity. The cell-associated recombinant minicellulosomes were found to be highly stable,

with a half-life of approximately 2 months at  $4^{\circ}\text{C}$  (data not shown).

**Functional analysis of the enzyme components in displayed minicellulosomes.** To examine whether the chimeric enzymes in the surface-displayed minicellulosomes were functional, three recombinant strains, CipA3-EGII, CipA3-CBHII, and CipA3-EGII-CBHII-BGL1 (Table 1), were tested to determine their abilities to hydrolyze amorphous cellulose (PASC). As shown in Fig. 4A, both strain CipA3-EGII and strain CipA3-CBHII released soluble reducing sugars from PASC, indicating that both EGII and CBHII in the recombinant minicellulosomes were functional. HPLC analysis of the hydrolysis products showed that CipA3-EGII released cellobiose and cellobiose as its main products, while only cellobiose was detected in the hydrolysis reaction mixture of strain CipA3-CBHII (data not shown). Although no reducing sugar was detected in the hydrolysis reaction mixture of strain CipA3-EGII-CBHII-BGL1, there was a significant reduction in the

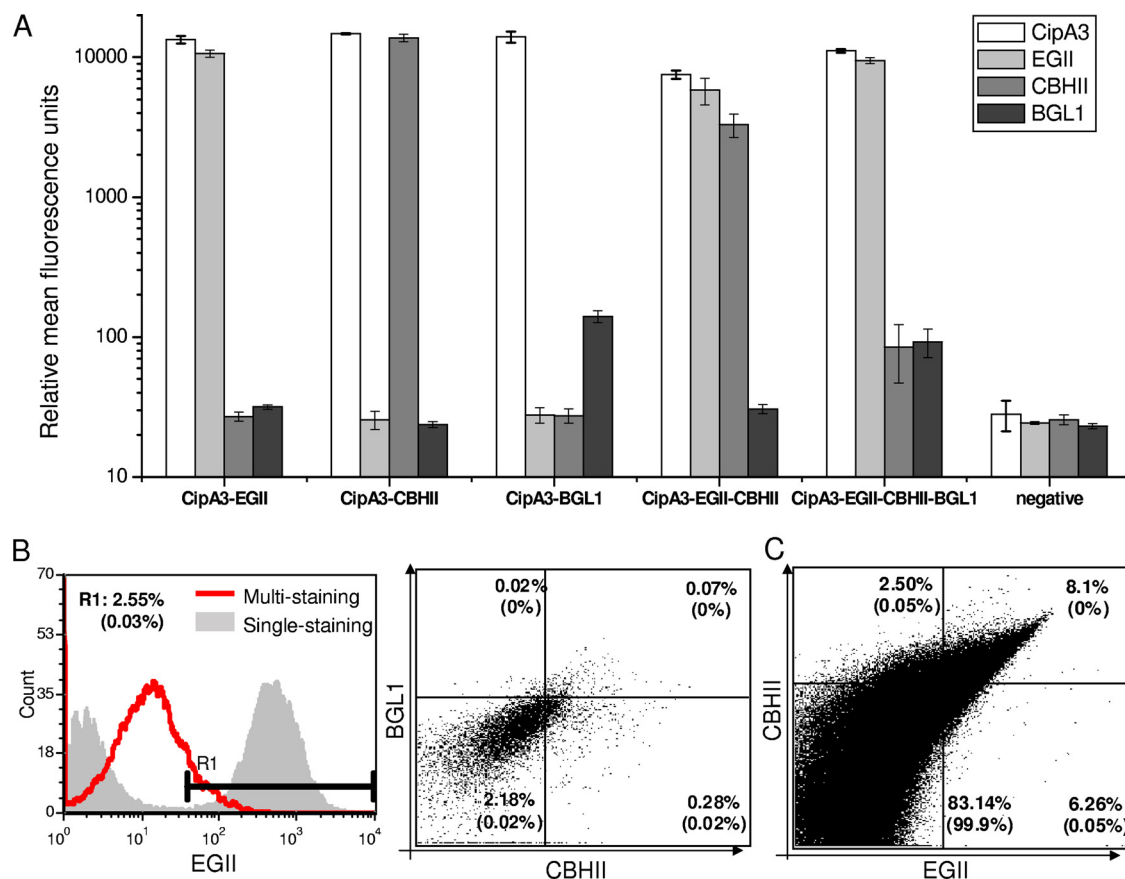


FIG. 3. Characterization of yeast surface-displayed minicellulosomes. (A) Level of display of all CipA3-based minicellulosomal components on the yeast cell surface. See Table 1 for the phenotype of each yeast strain. (B) Multi-antibody staining of strain CipA3-EGII-CBHII-BGL1. The multi-antibody staining showed significantly lower efficiency than single-antibody staining (left panel). The right panel was gated on the EGII<sup>+</sup> population shown by the R1 region in the left panel. (C) Multi-antibody staining of strain CipA3-EGII-CBHII. No gate was set, and the percentage of each population is shown in four quadrants. The corresponding percentages of the negative control are indicated in parentheses. The results were obtained in three independent experiments using three individual clones, and the averages and standard deviations are shown.

amount of the residual insoluble PASC (Fig. 4B), indicating that BGL1 was active. The activity of BGL1 was further confirmed by growth of strain CipA3-EGII-CBHII-BGL1 using cellobiose as the sole carbon source (Fig. 4C). In addition, the inability of strain CipA3-EGII-CBHII to grow on cellobiose excluded the possibility of endogenous BGL activity. Taken together, these data suggested that BGL1 was highly active and that the soluble oligosaccharides were quickly hydrolyzed by BGL1 to glucose, which was then immediately assimilated by yeast cells. Both HPLC analysis and a phenol-sulfuric acid assay showed that no PASC was hydrolyzed by the negative control strain (data not shown and Fig. 4). Taken together, these results demonstrated that all three chimeric enzymes in the minicellulosomes were active. The continuous degradation of PASC indicated that the surface-displayed cellulosomes were highly stable at 30°C (Fig. 4), and hydrolysis was complete after ~6 days for strain CipA3-EGII-CBHII-BGL1 (data not shown).

**Enhanced synergy of bifunctional and trifunctional minicellulosomes.** The recombinant yeast strains were tested to determine their abilities to hydrolyze amorphous cellulose (PASC) at 30°C. The number-average degrees of polymerization of PASC and Avicel were determined to be 190 and 192,

respectively, suggesting that the acid treatment process disrupted the supramolecular structure of Avicel without any significant acid hydrolysis. Compared to yeast strains displaying unifunctional minicellulosomes (i.e., CipA3-EGII and CipA3-CBHII), strain CipA3-EGII-CBHII displaying bifunctional minicellulosomes showed an increased rate of hydrolysis with PASC (Fig. 4A and B). Despite the dramatic decrease in the CBHII display level, the addition of a third enzyme, BGL1, in strain CipA3-EGII-CBHII-BGL1 further enhanced the hydrolysis efficiency (Fig. 4B). The maximum observed enhancement of activity was ~8.8-fold after ~24 h (Fig. 4B and Fig. 5), and then the enhancement decreased to ~2-fold and remained steady until completion of hydrolysis after ~144 h (data not shown).

To further examine whether the enhanced activity of bi- and trifunctional minicellulosomes was simply a result of enzyme-enzyme synergy or a combination of enzyme-enzyme synergy and enzyme proximity synergy (a characteristic feature of cellulosomes), two more recombinant yeast strains, CipA1-EGII-CBHII and CipA1-EGII-CBHII-BGL1, were constructed (Table 1). The use of miniscaffoldin CipA1 enabled simultaneous display of two or three types of unifunctional minicellulosomes that were spatially restricted on the cell surface, which allowed

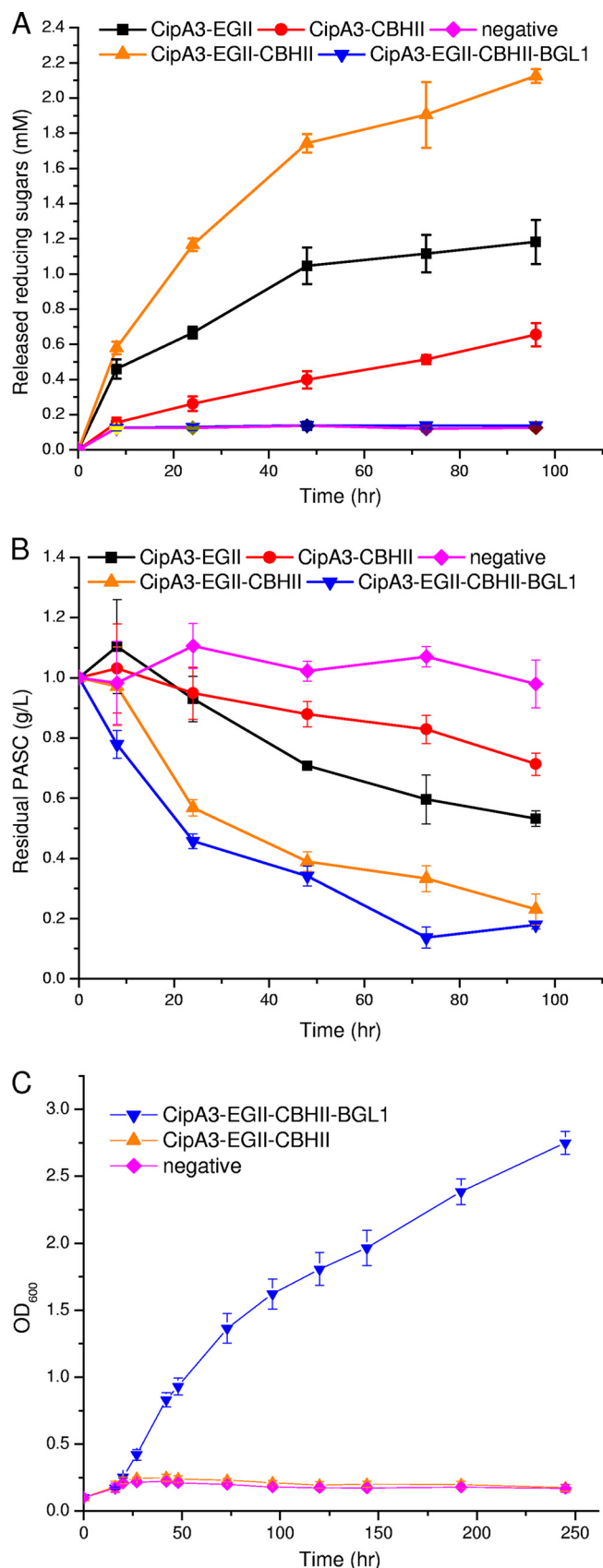


FIG. 4. (A and B) Functional analysis of surface-displayed minicellulosomes. Cells displaying different minicellulosomes were tested to

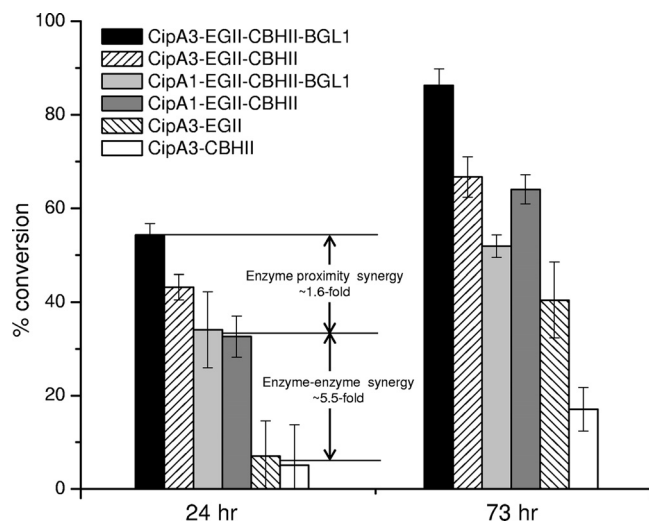


FIG. 5. Enhanced synergy of bifunctional and trifunctional minicellulosomes. The percentages of PASC conversion for six surface-engineered yeast strains were compared after 24 and 73 h. The differences between the CipA1-based minicellulosomes and the unifunctional minicellulosomes reflect the enzyme-enzyme synergy, while the differences between the CipA3- and CipA1-based minicellulosomes reflect the enzyme proximity synergy.

us to dissect the contributions of the two different synergisms (Fig. 1B). As shown in Fig. 5, both strain CipA1-EGII-CBHII and strain CipA1-EGII-CBHII-BGL1 clearly showed enzyme-enzyme synergy that resulted in activity that was ~5.5-fold higher than that of CipA3-EGII and CipA3-CBHII after 24 h. When the chimeric enzymes were brought into proximity on the miniscaffoldin CipA3, strains CipA3-EGII-CBHII and CipA3-EGII-CBHII-BGL1 showed additional ~1.3- and 1.6-fold-higher activities than the corresponding CipA1-strains, respectively. These results strongly suggested that the enhanced activity of the bi- and trifunctional minicellulosomes displayed on the yeast cell surface was a result of both enzyme-enzyme synergy and enzyme proximity synergy. Notably, the synergistic effect of BGL1 was more profound when BGL1 was in close proximity to EGII and CBHII (Fig. 5). As a result, although strain CipA3-EGII-CBHII-BGL1 showed much a lower level of CBHII display than strain CipA3-EGII-CBHII, the former strain maintained higher activity even after ~144 h, while the opposite result was obtained for the CipA1-based strains.

**Direct conversion of cellulose to ethanol.** Direct production of ethanol from PASC was carried out anaerobically in a serum bottle using strain CipA3-EGII-CBHII-BGL1 displaying trifunctional minicellulosomes. Since this strain did not show sustained growth on PASC (data not shown), cells were pre-

determine their abilities to hydrolyze PASC. The concentrations of (A) released reducing sugars and (B) residual PASC were plotted over time. (C) Time courses of the cell growth using cellobiose as the sole carbon source. Samples were taken at the time points indicated, and the optical density at 600 nm was measured using a UV-visible spectrometer. All data were obtained from triplicate experiments, and the averages and standard deviations are shown.

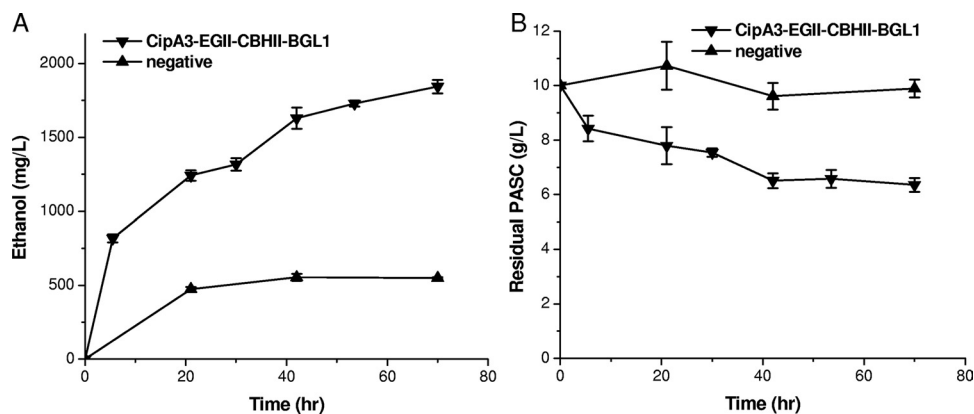


FIG. 6. Simultaneous saccharification and fermentation of PASC to ethanol by yeast strain CipA3-EGII-CBHII-BGL1 displaying trifunctional minicellulosomes. The concentrations of (A) ethanol and (B) residual PASC over time are plotted. Yeast strain HZ1901 was used as a negative control.

cultured, induced, and then resuspended in fermentation medium to an  $OD_{600}$  of 50. As shown in Fig. 6, PASC consumption by strain CipA3-EGII-CBHII-BGL1 started without a time lag, and within the first 6 h of fermentation, the ethanol titer quickly reached  $\sim 1$  g/liter. After this, the rate of ethanol production decreased, and the titer reached  $\sim 1.8$  g/liter after 70 h. The decrease in the rate of ethanol production was probably due to the increase in the pH of the fermentation medium to  $\sim 7$ , at which the enzyme activity was not optimal. The yield was 0.31 g of ethanol produced per g of PASC consumed, which corresponded to  $\sim 62\%$  of the theoretical yield. The ethanol produced by the negative control strain was not a result of PASC fermentation but resulted from YP medium fermentation (Fig. 6B) since the same amount of ethanol was also observed using unsupplemented YP medium (data not shown).

## DISCUSSION

CBP is one of the most promising processing strategies for cost-effective cellulosic ethanol production, and the development of a whole-cell biocatalyst that can efficiently ferment cellulosic biomass to ethanol is the key to its success (3, 23, 24). Much effort has been devoted to engineering of *S. cerevisiae* for CBP because *S. cerevisiae* has many superior traits, including high ethanol productivity, yield, and tolerance; robustness in industrial fermentation; a wide variety of genetic engineering tools; and generally regarded as safe status (36). One of the key challenges of using *S. cerevisiae* as a CBP host is to confer the ability to degrade cellulose rapidly into glucose. In nature, cellulolytic anaerobes have evolved an intricate multienzyme complex, the cellulosome, to efficiently break down the plant cell wall. The degradative potential of the cellulosome has sparked great interest in producing and engineering recombinant or designer cellulosomes for biotechnological and bioenergy applications (3, 28). In this study, we successfully displayed two miniscaffoldins, CipA3 and CipA1, on the yeast cell surface (Fig. 1 and 2), which served as anchor proteins to assemble a series of uni-, bi-, and trifunctional minicellulosomes (Fig. 3 and Table 1). All of the recombinant minicellulosomes were extremely stable and showed hydrolytic activity

with amorphous cellulose (Fig. 4 and 5). To our knowledge, this is the first successful report of production of functional multiple-enzyme-containing minicellulosomes *in vivo*. More importantly, recombinant yeast cells displaying trifunctional minicellulosomes on the surface synergistically hydrolyzed amorphous cellulose to glucose and efficiently fermented it to ethanol with a titer of  $\sim 1.8$  g/liter (Fig. 6). These results demonstrated the feasibility of combining designer cellulosomes and CBP, two of the most promising technologies for future biorefineries.

A recent study showed that synergistic hydrolysis of amorphous cellulose could be achieved by simply codisplaying three cellulases on the yeast cell surface as individual fusion proteins with the C-terminal half of  $\alpha$ -agglutinin (16). The experimental design in this previous study resembled the CipA1 strains created in our study, in which the enzymes were spatially distributed on the yeast cell surface and thus no enzyme proximity synergy could be incorporated using the display system. In addition, C-terminal fusion of the  $\alpha$ -agglutinin impaired enzyme activity since no CBHII activity with PASC was detected and no EGII activity was detected within 10 h (16). In contrast, when CBHII or EGII was displayed on cell surface through cohesin-dockerin interactions, both enzymes showed higher activity with PASC (Fig. 4). Bringing the two enzymes in close proximity on a miniscaffoldin, CipA3, further enhanced the activity; 1.9 mM reducing sugars (this study) instead of 1.3 mM reducing sugars (16) was released from PASC after  $\sim 72$  h. These results clearly showed the advantage of engineering cellulolytic yeast strains through surface display of minicellulosomes to incorporate their synergistic hydrolytic activity.

In another study, which was published when this paper was under review, Tsai et al. also successfully displayed a functional miniscaffoldin on the yeast cell surface (34). While both that study and the work described here showed that there was synergistic hydrolysis and direct fermentation of PASC to ethanol, there is a significant difference between the engineered yeast strains in terms of consolidated bioprocessing. Tsai et al. (34) did not demonstrate that the yeast cells were capable of synthesizing functional minicellulosomes. In fact, the recombinant yeast strain in their study was not truly cellulolytic and required *in vitro* loading of the enzyme components, which

were produced in *E. coli*, onto the scaffoldin. In contrast, we showed that, by coexpressing a miniscaffoldin and three types of cellulases, yeast cells could be made cellulolytic, a critical requirement for using yeast cells in consolidated bioprocessing (24). Therefore, we believe that the yeast strain described in this study (Fig. 1) represents a better engineering platform for development of CBP-enabling microorganisms. In addition, the recombinant yeast cells developed in this study could also be a useful tool for studying and engineering the synergisms of cellulosomes. The mechanisms responsible for the enhanced activity of cellulosomes were poorly understood until recently, when precise control of cellulosomal composition and arrangement was made possible by construction of designer cellulosome chimeras *in vitro* (14, 15). In theory, such chimeras can be readily assembled on the yeast cell surface by replacing the miniscaffoldin CipA3 used in this study with a chimeric scaffoldin containing divergent cohesin modules and replacing the dockerin domains with cognate specificity. Since the display method described here allows production of all cellulosomal components *in vivo*, it avoids the labor-intensive protein purification step. In addition, any of the cellulosomal components could be easily swapped with components of interest using the DNA assembler method, which allows fast assembly of DNA fragments into a large molecule in a single transformation step (33). Therefore, the *in vivo* method described here is a convenient and robust means of producing and studying cellulosomes for biotechnological and industrial applications.

In this study, we dissected the contributions of enzyme-enzyme synergy and enzyme proximity synergy to the enhanced activity of yeast surface-displayed minicellulosomes. Because yeast surface-displayed unifunctional minicellulosomes were not capable of two-dimensional diffusion (5), they were spatially distributed on the yeast cell surface and exhibited little, if any, enzyme proximity synergy (Fig. 1 and 5). The observed ~8.8-fold enhanced activity of the trifunctional minicellulosome was a result of both enzyme-enzyme synergy and enzyme proximity synergy, which accounted for ~63% and ~37% of the overall synergy, respectively. It was also observed that the synergistic effect of BGL1 was more profound when BGL1 was in close proximity to EGII and CBHII, indicating that there was a higher local cellobiose concentration near the surface of the PASC reacting site that inhibited the activity of EGII and/or CBHII.

More importantly, we successfully demonstrated simultaneous saccharification and fermentation of amorphous cellulose to ethanol using a yeast strain displaying trifunctional minicellulosomes. However, the direct conversion of crystalline cellulose to ethanol remains a challenging task. In theory, the trifunctional minicellulosomes constructed in this study should meet the minimum requirement for crystalline cellulose fermentation. Indeed, when we tested strain CipA3-EGII-CBHII-BGL1 to determine its ability to ferment Avicel, it did produce ethanol, but at an extremely low level (the titer after about 5 days was ~0.4 g/liter) (data not shown). Such slow catalysis and low fermentation efficiency could be potentially improved by increasing the enzyme display levels and/or activity. Concomitantly, cellulosomes with higher levels of complexity could be assembled to further boost synergy. Although such studies are in progress, the results pre-

sented here underscore the potential of engineering yeast as a CBP platform organism using surface display of cellulosomes.

#### ACKNOWLEDGMENTS

We thank Nikhil U. Nair for helpful discussions and members of the Zhao laboratory for critical comments on the manuscript. We also thank Barbara Pilas and Bernard Montez at the Biotechnology Center and Alexander Ulanov at the Metabolomics Center of the University of Illinois for technical assistance.

This work was supported by the Centennial Endowed Chair Fund of the Department of Chemical and Biomolecular Engineering at the University of Illinois at Urbana-Champaign.

#### REFERENCES

- Arai, T., S. Matsuoka, H. Y. Cho, H. Yukawa, M. Inui, S. L. Wong, and R. H. Doi. 2007. Synthesis of *Clostridium cellulovorans* minicellulosomes by intercellular complementation. *Proc. Natl. Acad. Sci. U. S. A.* **104**:1456–1460.
- Bayer, E. A., J. P. Belaich, Y. Shoham, and R. Lamed. 2004. The cellulosomes: multienzyme machines for degradation of plant cell wall polysaccharides. *Annu. Rev. Microbiol.* **58**:521–554.
- Bayer, E. A., R. Lamed, and M. E. Himmel. 2007. The potential of cellulases and cellulosomes for cellulosic waste management. *Curr. Opin. Biotechnol.* **18**:237–245.
- Beguín, P., P. Cornet, and J. P. Aubert. 1985. Sequence of a cellulase gene of the thermophilic bacterium *Clostridium thermocellum*. *J. Bacteriol.* **162**:102–105.
- Boder, E. T., J. R. Bill, A. W. Nields, P. C. Marrack, and J. W. Kappler. 2005. Yeast surface display of a noncovalent MHC class II heterodimer complexed with antigenic peptide. *Biotechnol. Bioeng.* **92**:485–491.
- Boder, E. T., and K. D. Wittrup. 1997. Yeast surface display for screening combinatorial polypeptide libraries. *Nat. Biotechnol.* **15**:553–557.
- Caspi, J., D. Irwin, R. Lamed, Y. Li, H. P. Fierobe, D. B. Wilson, and E. A. Bayer. 2008. Conversion of *Thermobifida fusca* free exoglucanases into cellulosomal components: comparative impact on cellulose-degrading activity. *J. Biotechnol.* **135**:351–357.
- Cho, H. Y., H. Yukawa, M. Inui, R. H. Doi, and S. L. Wong. 2004. Production of minicellulosomes from *Clostridium cellulovorans* in *Bacillus subtilis* WB800. *Appl. Environ. Microbiol.* **70**:5704–5707.
- Clements, J. M., G. H. Catlin, M. J. Price, and R. M. Edwards. 1991. Secretion of human epidermal growth factor from *Saccharomyces cerevisiae* using synthetic leader sequences. *Gene* **106**:267–271.
- Cosgrove, D. J. 2005. Growth of the plant cell wall. *Nat. Rev. Mol. Cell Biol.* **6**:850–861.
- Demain, A. L., M. Newcomb, and J. H. Wu. 2005. Cellulase, clostridia, and ethanol. *Microbiol. Mol. Biol. Rev.* **69**:124–154.
- Den Haan, R., S. H. Rose, L. R. Lynd, and W. H. van Zyl. 2007. Hydrolysis and fermentation of amorphous cellulose by recombinant *Saccharomyces cerevisiae*. *Metab. Eng.* **9**:87–94.
- Doi, R. H. 2008. Cellulases of mesophilic microorganisms: cellulosome and noncellulosome producers. *Ann. N. Y. Acad. Sci.* **1125**:267–279.
- Fierobe, H. P., E. A. Bayer, C. Tardif, M. Czjzek, A. Mechaly, A. Belaich, R. Lamed, Y. Shoham, and J. P. Belaich. 2002. Degradation of cellulose substrates by cellulosome chimeras. Substrate targeting versus proximity of enzyme components. *J. Biol. Chem.* **277**:49621–49630.
- Fierobe, H. P., F. Mingardon, A. Mechaly, A. Belaich, M. T. Rincon, S. Pages, R. Lamed, C. Tardif, J. P. Belaich, and E. A. Bayer. 2005. Action of designer cellulosomes on homogeneous versus complex substrates: controlled incorporation of three distinct enzymes into a defined trifunctional scaffoldin. *J. Biol. Chem.* **280**:16325–16334.
- Fujita, Y., J. Ito, M. Ueda, H. Fukuda, and A. Kondo. 2004. Synergistic saccharification, and direct fermentation to ethanol, of amorphous cellulose by use of an engineered yeast strain codisplaying three types of cellulolytic enzyme. *Appl. Environ. Microbiol.* **70**:1207–1212.
- Fujita, Y., S. Takahashi, M. Ueda, A. Tanaka, H. Okada, Y. Morikawa, T. Kawaguchi, M. Arai, H. Fukuda, and A. Kondo. 2002. Direct and efficient production of ethanol from cellulosic material with a yeast strain displaying cellulolytic enzymes. *Appl. Environ. Microbiol.* **68**:5136–5141.
- Gerngross, U. T., M. P. Romaniec, T. Kobayashi, N. S. Huskisson, and A. L. Demain. 1993. Sequencing of a *Clostridium thermocellum* gene (cipA) encoding the cellulosomal SL-protein reveals an unusual degree of internal homology. *Mol. Microbiol.* **8**:325–334.
- Himmel, M. E., S. Y. Ding, D. K. Johnson, W. S. Adney, M. R. Nimlos, J. W. Brady, and T. D. Foust. 2007. Biomass recalcitrance: engineering plants and enzymes for biofuels production. *Science* **315**:804–807.
- Horton, R. M., Z. L. Cai, S. N. Ho, and L. R. Pease. 1990. Gene splicing by overlap extension: tailor-made genes using the polymerase chain reaction. *Biotechniques* **8**:528–535.
- Lu, Y., Y. H. Zhang, and L. R. Lynd. 2006. Enzyme-microbe synergy during

- cellulose hydrolysis by *Clostridium thermocellum*. Proc. Natl. Acad. Sci. U. S. A. **103**:16165–16169.
22. Lynd, L. R., M. S. Laser, D. Bransby, B. E. Dale, B. Davison, R. Hamilton, M. Himmel, M. Keller, J. D. McMillan, J. Sheehan, and C. E. Wyman. 2008. How biotech can transform biofuels. Nat. Biotechnol. **26**:169–172.
  23. Lynd, L. R., W. H. van Zyl, J. E. McBride, and M. Laser. 2005. Consolidated bioprocessing of cellulosic biomass: an update. Curr. Opin. Biotechnol. **16**:577–583.
  24. Lynd, L. R., P. J. Weimer, W. H. van Zyl, and I. S. Pretorius. 2002. Microbial cellulose utilization: fundamentals and biotechnology. Microbiol. Mol. Biol. Rev. **66**:506–577.
  25. Miller, C. A., III, M. A. Martinat, and L. E. Hyman. 1998. Assessment of aryl hydrocarbon receptor complex interactions using pBEVY plasmids: expression vectors with bi-directional promoters for use in *Saccharomyces cerevisiae*. Nucleic Acids Res. **26**:3577–3583.
  26. Mingardon, F., A. Chanal, A. M. Lopez-Contreras, C. Dray, E. A. Bayer, and H. P. Fierobe. 2007. Incorporation of fungal cellulases in bacterial minicellulosomes yields viable, synergistically acting cellulolytic complexes. Appl. Environ. Microbiol. **73**:3822–3832.
  27. Mingardon, F., S. Perret, A. Belaich, C. Tardif, J. P. Belaich, and H. P. Fierobe. 2005. Heterologous production, assembly, and secretion of a minicellulosome by *Clostridium acetobutylicum* ATCC 824. Appl. Environ. Microbiol. **71**:1215–1222.
  28. Nordon, R. E., S. J. Craig, and F. C. Foong. 2009. Molecular engineering of the cellulosome complex for affinity and bioenergy applications. Biotechnol. Lett. **31**:465–476.
  29. Pages, S., A. Belaich, J. P. Belaich, E. Morag, R. Lamed, Y. Shoham, and E. A. Bayer. 1997. Species-specificity of the cohesin-dockerin interaction between *Clostridium thermocellum* and *Clostridium cellulolyticum*: prediction of specificity determinants of the dockerin domain. Proteins **29**:517–527.
  30. Parekh, R., K. Forrester, and D. Witttrup. 1995. Multicopy overexpression of bovine pancreatic trypsin inhibitor saturates the protein folding and secretory capacity of *Saccharomyces cerevisiae*. Protein Expr. Purif. **6**:537–545.
  31. Percival Zhang, Y. H., M. E. Himmel, and J. R. Mielenz. 2006. Outlook for cellulase improvement: screening and selection strategies. Biotechnol. Adv. **24**:452–481.
  32. Rubin, E. M. 2008. Genomics of cellulosic biofuels. Nature **454**:841–845.
  33. Shao, Z., H. Zhao, and H. Zhao. 2009. DNA assembler, an *in vivo* genetic method for rapid construction of biochemical pathways. Nucleic Acids Res. **37**:e16.
  34. Tsai, S. L., J. Oh, S. Singh, R. Chen, and W. Chen. 2009. Functional assembly of minicellulosomes on the *Saccharomyces cerevisiae* cell surface for cellulose hydrolysis and ethanol production. Appl. Environ. Microbiol. **75**:6087–6093.
  35. U.S. Department of Energy Office of Science and Office of Energy Efficiency and Renewable Energy. 2006. Breaking the biological barriers to cellulosic ethanol: a joint research agenda. Publication DOE/SC-0095. U.S. Department of Energy Office of Science and Office of Energy Efficiency and Renewable Energy, Washington, DC. <http://genomicscience.energy.gov/biofuels/b2bworkshop.shtml>.
  36. van Zyl, W. H., L. R. Lynd, R. den Haan, and J. E. McBride. 2007. Consolidated bioprocessing for bioethanol production using *Saccharomyces cerevisiae*. Adv. Biochem. Eng. Biotechnol. **108**:205–235.
  37. Wang, W. K., K. Kruus, and J. H. Wu. 1993. Cloning and DNA sequence of the gene coding for *Clostridium thermocellum* cellulase Ss (CelS), a major cellulosome component. J. Bacteriol. **175**:1293–1302.
  38. Wen, F., O. Esteban, and H. Zhao. 2008. Rapid identification of CD4<sup>+</sup> T-cell epitopes using yeast displaying pathogen-derived peptide library. J. Immunol. Methods **336**:37–44.
  39. Wen, F., N. U. Nair, and H. Zhao. 2009. Protein engineering in designing tailored enzymes and microorganisms for biofuels production. Curr. Opin. Biotechnol. **20**:412–419.
  40. Wood, T., and K. Bhat. 1988. Methods for measuring cellulase activities. Methods Enzymol. **160**:87–112.
  41. Wyman, C. E. 2007. What is (and is not) vital to advancing cellulosic ethanol. Trends Biotechnol. **25**:153–157.
  42. Zhang, Y. H., J. Cui, L. R. Lynd, and L. R. Kuang. 2006. A transition from cellulose swelling to cellulose dissolution by o-phosphoric acid: evidence from enzymatic hydrolysis and supramolecular structure. Biomacromolecules **7**:644–648.
  43. Zhang, Y. H., and L. R. Lynd. 2005. Determination of the number-average degree of polymerization of cellobextrins and cellulose with application to enzymatic hydrolysis. Biomacromolecules **6**:1510–1515.